NeuroImage 268 (2023) 119893

Contents lists available at ScienceDirect

NeuroImage

journal homepage: www.elsevier.com/locate/neuroimage

Cortical encoding of rhythmic kinematic structures in biological motion

Li Shen [a,b,c], Xiqian Lu [a,b,c], Xiangyong Yuan [a,b,c], Ruichen Hu [a,b,c], Ying Wang [a,b,c,*], Yi Jiang [a,b,c]

[a] State Key Laboratory of Brain and Cognitive Sciences, CAS Center for Excellence in Brain Science and Intelligence Technology, Institute of Psychology, Chinese Academy of Sciences, Beijing 100101, China
[b] Department of Psychology, University of Chinese Academy of Sciences, Beijing 100049, China
[c] Chinese Institute for Brain Research, Beijing 102206, China

ARTICLE INFO

Keywords:
Biological motion
Visual perception
Kinematic
Rhythmic
Neural oscillations
Cortical tracking

ABSTRACT

Biological motion (BM) perception is of great survival value to human beings. The critical characteristics of BM information lie in kinematic cues containing rhythmic structures. However, how rhythmic kinematic structures of BM are dynamically represented in the brain and contribute to visual BM processing remains largely unknown. Here, we probed this issue in three experiments using electroencephalogram (EEG). We found that neural oscillations of observers entrained to the hierarchical kinematic structures of the BM sequences (i.e., step-cycle and gait-cycle for point-light walkers). Notably, only the cortical tracking of the higher-level rhythmic structure (i.e., gait-cycle) exhibited a BM processing specificity, manifested by enhanced neural responses to upright over inverted BM stimuli. This effect could be extended to different motion types and tasks, with its strength positively correlated with the perceptual sensitivity to BM stimuli at the right temporal brain region dedicated to visual BM processing. Modeling results further suggest that the neural encoding of spatiotemporally integrative kinematic cues, in particular the opponent motions of bilateral limbs, drives the selective cortical tracking of BM information. These findings underscore the existence of a cortical mechanism that encodes periodic kinematic features of body movements, which underlies the dynamic construction of visual BM perception.

1. Introduction

Rhythms are central to life and pervasive in human behaviors. The neural oscillations in our working brains are rhythmic (Hutcheon & Yarom, 2000). The sounds and actions we produce, such as the words we utter and the movements we make, also convey rhythmic signals (Kotz et al., 2018). There has been a growing interest in exploring how oscillatory brain activities dynamically encode rhythmic structures in human speech and language-related behaviors (Brookshire et al., 2017; Ding et al., 2016, 2017; Keitel et al., 2018; Luo and Ding, 2020; Riecke et al., 2018). However, it remains largely unknown whether and how neural oscillations encode non-verbal rhythmic signals in human movements.

The current study focused on the neural encoding of biological motion (BM), particularly the bodily movements of human beings, which deliver a wealth of biologically and socially relevant information and involve distinct mechanisms from that for nonbiological motion stimuli (Blake and Shiffrar, 2007; Giese and Poggio, 2003; Hirai and Senju, 2020; Pavlova, 2012; Yovel and O'Toole, 2016). The kinematics of BM can be isolated by point-light animations that consist of small light tokens placed at the major joints of a human actor (Johansson, 1973). Crucially, some basic forms of BM signals convey characteristic rhythmic structures derived from kinematic cues, which have been linked to the specialized visual processing of BM information. Take locomotion as an example: the forward motion of each step, generated by either the left or the right foot, occurs recurrently to form a basic-level rhythmic structure (i.e., step cycle), and the alternating movements of the two feet repeat periodically to specify a higher-level rhythmic structure (i.e., gait cycle). A substantial difference between these structures is that the gait cycle conveys information that the step cycle does not have, e.g., the phase relation between the limbs, which provides critical features for the recognition of human motion (Booth et al., 2002; Casile and Giese, 2005; Giese and Poggio, 2003). A recent study showed that observers' perceptual sensitivity to the point-light human BM fluctuates over time in a sinusoidal pattern that mimics the rhythmic structures of the BM stimuli (Thurman and Grossman, 2008). Notably, the extraction of these rhythmic structures relies on the spatiotemporal summation of BM information (Casile and Giese, 2005; Giese and Poggio, 2003; Neri et al., 1998). Meanwhile, the duration of motion cycles limits the temporal summation of BM but not translational or apparent motion (Beintema et al., 2006; Cai et al., 2011; Faivre and Koch, 2014; Neri et al., 1998), suggesting that BM processing may engage a special-

* Corresponding author at: State Key Laboratory of Brain and Cognitive Sciences, CAS Center for Excellence in Brain Science and Intelligence Technology, Institute of Psychology, Chinese Academy of Sciences, Beijing 100101, China.
E-mail address: wangying@psych.ac.cn (Y. Wang).

https://doi.org/10.1016/j.neuroimage.2023.119893.
Received 28 July 2022; Received in revised form 4 January 2023; Accepted 20 January 2023
Available online 21 January 2023.

ized temporal summation mechanism driven by rhythmic kinematic cues.

Here, we investigated the dynamic neural encoding of the rhythmic kinematic structures in BM stimuli and sought to reveal the underlying spatiotemporal summation mechanism. In three EEG experiments, we examined whether observers' neural oscillations entrain to the hierarchical kinematic structures in BM stimuli (e.g., the step cycle and the gait cycle for a walker), and if so, whether such neural entrainment effect reflects the specialized visual processing of BM information. To this end, we included both upright and inverted BM stimuli. Inversion disrupts the distinctive kinematic features of BM (e.g., gravity-compatible ballistic movements) and can significantly impair BM processing (Chang and Troje, 2008; Grossman and Blake, 2001; Simion et al., 2008; Troje and Westhoff, 2006; Vallortigara and Regolin, 2006; Wang et al., 2010; Wang et al., 2022), whereas it does not change the basic visual properties and complexity of the stimuli, including the rhythmic signals generated by low-level motion cues. Therefore, the inversion effect has long been regarded as a marker of the specificity of BM processing, especially when dealing with the visual analysis of kinematic cues (Bardi et al., 2014; Troje and Westhoff, 2006; Wang et al., 2014; Wang and Jiang, 2012), and is expected to reflect the BM-specific neural encoding process in our study. We found that while neural oscillations entrained to both basic- and higher-level rhythmic structures in BM signals, only the neural responses induced by higher-level structures were selectively enhanced for upright BM to support a BM-specific neural representation. These results can be generalized to different stimuli (Walk in Experiment 1; Jump in Experiment 2) and tasks (speed-change-detection in Experiments 1 & 2a; transient-variation-detection in Experiment 2b).

We further explored the encoding mechanism underlying the BM-specific neural responses via computational modeling. In particular, we assessed the contributions of two spatiotemporal summation mechanisms to the orientation-dependent visual processing of BM information: one pertains to the neural encoding of accumulating motion signals across joints (i.e., additive signals), the other associates with the neural representation of the relative opponent motion of bilateral limbs (i.e., integrative signals). We estimated the weights of these signals by fitting them to the observed neural oscillation activity in the upright and inverted conditions, respectively. If the cortical tracking of a given signal underpins the specialized visual processing of BM information, this signal would be expected to have a larger weight in the upright than in the inverted condition.

2. Materials and methods

2.1. Participants

A total of 40 participants with normal or corrected-to-normal vision took part in this study, 20 (11 female, mean age ± SD = 21.75 ± 2.10 years) in Experiment 1 and the other 20 (10 female, mean age ± SD = 21.20 ± 2.14 years) in Experiment 2. None had neurological or psychiatric disorders. They were naïve to the purpose of the study and gave informed consent according to procedures and protocols approved by the institutional review board of the Institute of Psychology, Chinese Academic of Sciences.

2.2. Stimuli

Two types of BM stimuli, Walk (3.05°×5.47°) and Jump (3.22°×5.97°), were used in Experiment 1 (Fig. 1, upper panel) and 2 (Fig. 1, lower panel), respectively. The BM stimuli consisted of 13 point-light dots attached to the major joints and the head of an actor (Vanrie and Verfaillie, 2004). The point-light stimuli did not translate on the screen and looked like a person walking on a treadmill or performing jumping jacks at the same position. A complete walk cycle lasted 1 s and was repeated 6 times to form a 6 s walking sequence (walk cycle frequency: 1 Hz). A jump cycle lasted 1.2 s and was repeated 5 times within a 6 s jumping sequence (jump cycle frequency: 0.83 Hz).

The inverted BM stimuli were created by mirror-flipping the upright BM vertically. Inversion disrupts the distinctive kinematic features (e.g., gravity-compatible ballistic movements) of BM stimuli but does not change the rhythmic signals (Simion et al., 2008; Troje and Westhoff, 2006; Vallortigara and Regolin, 2006; Wang et al., 2014; Wang and Jiang, 2012, 2022). All stimuli were rendered white against a gray background and displayed using MATLAB together with the Psychophysics Toolbox (Brainard, 1997; Pelli, 1997).

2.3. Procedure and task

All the Experiments were conducted in an acoustically dampened and electromagnetically shielded chamber. Participants sat 60 cm from a CRT monitor (1280×1024,60 Hz), with their heads held stationary on a chinrest.

In Experiment 1, each trial (Fig. 1, middle panel) began with a white fixation cross (0.42° × 0.42°) displayed at the center of a gray background for a random duration (0.8 s to 1 s). Subsequently, a point-light walker walking toward left or right at a constant walking cycle frequency (1 Hz) was presented for 6 s. To maintain observers' attention, 17–23% of the trials were randomly selected as catch trials, in which the speed of the walker changed one or two times throughout the trial. 'One time' indicates the speed of the walker becomes either faster (1.33 Hz) or slower (0.80 Hz) and remains unchanged until the walker disappears. 'Two times' indicates the speed of the walker becomes faster or slower and returns to its original speed after 2–2.5 s. Participants were required to detect and report the number of changes (0, 1, or 2) via keypresses as accurately as possible when the point-light display was replaced by a red fixation (i.e., speed detection task, SD task). The next trial started 2–3 s after the response. Each participant completed 6 practice trials to get familiar with the task. In the formal experiment, they completed two experimental blocks, one for the upright BM condition, the other for the inverted BM condition. The order of the blocks was counterbalanced across participants. Each block consisted of 52 experimental trials without speed changes and 10–15 catch trials, resulting in a total of 124–134 trials.

The procedure of Experiment 2a & 2b was identical to that of Experiment 1 except for the following differences. First, the stimuli were point light jumpers whose facing directions were deflected to the left or right by 22.5° from the central axis in the vertical plane. Second, the frequency of the jump cycle was 0.83 Hz and might change to 0.57 Hz or 1.67 Hz in the catch trials of Experiment 2a, where participants performed the SD task. In Experiment 2b, participants were required to perform a frequency-irrelevant variation detection task (VD task). In this task, a random one of the five jump cycles was temporally scrambled, leading to a transient variation in the catch trials. Participants had to judge whether a variation occurred or not.

2.4. EEG recording

EEG was recorded at 1000 Hz using a SynAmps^2 NeuroScan amplifier System with 64 Ag-Agcl electrodes placed on the scalp according to the international 10–20 system. Horizontal and vertical eye movements were measured via four additional electrodes (HEOG and VEOG) placed on the outer canthus of each eye and the inferior and superior areas of the left orbit. Impedances were kept below 5kΩ for all electrodes.

2.5. EEG analysis

Preprocessing. The catch trials were excluded from EEG analysis. All preprocessing and analysis were performed using the EEGLAB toolbox (Delorme and Makeig, 2004) in the MATLAB environment. EEG recordings were down-sampled to 100 Hz, band pass-filtered between 0.1 and

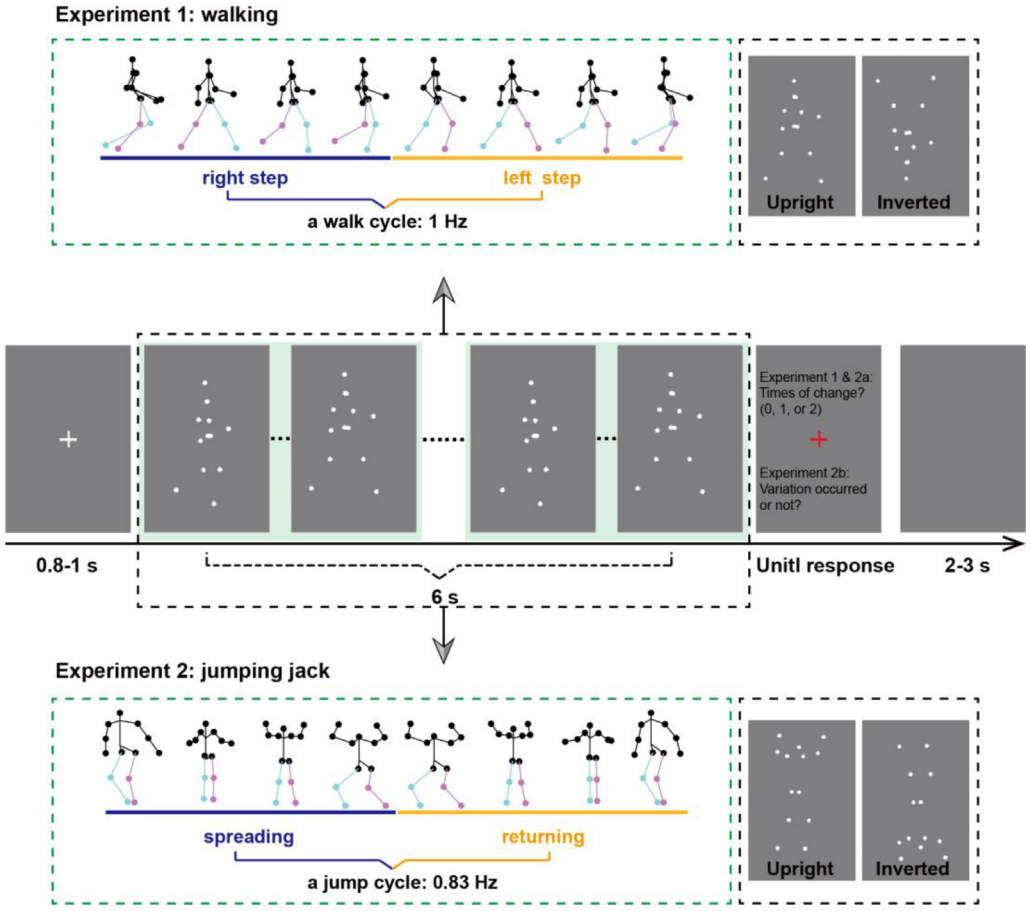

Fig. 1. Illustrations of visual stimuli and experimental procedures. The upper and lower panels depict the key frames from one cycle of the point-light walker and point-light jumper sequences, respectively. The colors of dots and lines between dots are used for illustration only and not shown in the formal experiment. The middle panel shows the experimental procedure. Each trial started with an 0.8–1 s fixation, followed by a point-light walker or jumper present for 6 s. 17–23% of the trials were catch trials, in which the speed of the BM stimuli randomly changed one or two times (Experiment 1 & 2a) or a transient variation occurred (Experiment 2b). No change or variation occurred in the experimental trials. Observers were required to report the times of changes occurred or whether the variation occurred or not when the red fixation was present after the BM stimuli disappeared. After the response, a blank screen appeared for 2–3 s.

30 Hz, and then segmented into a series of epochs starting at the onset of the stimuli and lasting 6 s. The epochs were visually inspected, and trials contaminated with excessive noise were excluded from the analysis. There was no difference between the upright and inverted conditions in terms of the total number of accepted epochs (means > 90%, *ps* > 0.38). After trial rejection, an independent component analysis (Jung et al., 2000) based on the Runica algorithm (Bell and Sejnowski, 1995; Makeig, 2002) was performed to remove eye and cardiac artifacts. For each participant, the cleaned data were re-referenced to the average mastoids (M1 and M2). The EEG recording during the first second of each trial was excluded to mitigate the influence of stimulus-onset evoked activity on EEG spectral decomposition (Nozaradan et al., 2012). After that, the EEG signals were averaged across trials for each participant in each condition.

Frequency-Domain Analysis. We converted the averaged waveforms from the temporal domain to the spectral domain using Fast Fourier Transform (FFT) with zero paddings (600). It resulted in a frequency resolution of 0.167 Hz, i.e., 1/6 Hz, which is sufficient for observing neural responses around the frequency of the rhythmic BM structures (1 Hz and 0.83 Hz). A Hanning window was applied when performing FFT to reduce spectral leakage. Power spectra were calculated as the squared amplitude and then converted to decibel scale (i.e., 10*log10). To remove the 1/f trend of the response power spectrum, the response power at each frequency was normalized by subtracting the average power measured at the neighboring frequency bins (two bins on each side, 0.33 Hz) from the power at each frequency (Ding et al., 2017; Lenc et al., 2018; Nozaradan et al., 2012). The power was calculated separately for each electrode (except for electrooculogram channels), participant, and condition.

Statistical analysis of EEG data. For each condition (Upright and Inverted), the significant neural entrainment effect or spectral peak at each target frequency (1 & 2 Hz for Walk; 0.83 & 1.67 Hz for Jump) was examined by contrasting the normalized response power at the target frequency against zero based on a two-sided *t*-test. A cluster-based permutation test with 1000 randomizations was used to control for multiple comparisons across channels (excluding the electrooculogram channels) and identify the spatial distribution of the significant cluster (Kayser et al., 2015; Maris and Oostenveld, 2007). The permutation test was performed based on the MATLAB toolbox FieldTrip (Oostenveld et al., 2011). We clustered data across channel neighborhoods with an average size of 6.5 channels determined by triangulated sensor proximity (function ft_prepara_neighbours, method 'triangulation'). A type 1 error probability of less than 0.05 was ensured for all clusters. To further evaluate the BM-specific cortical responses, we contrasted the entrainment effect between the upright and inverted conditions using a similar cluster-based permutation test. Power at the electrode clusters showing a significant inversion effect was averaged to depict the power spectrum. Finally, we adopted the Pearson correlation analysis and the cluster-based permutation statistics to assess whether interindividual differences in the BM-

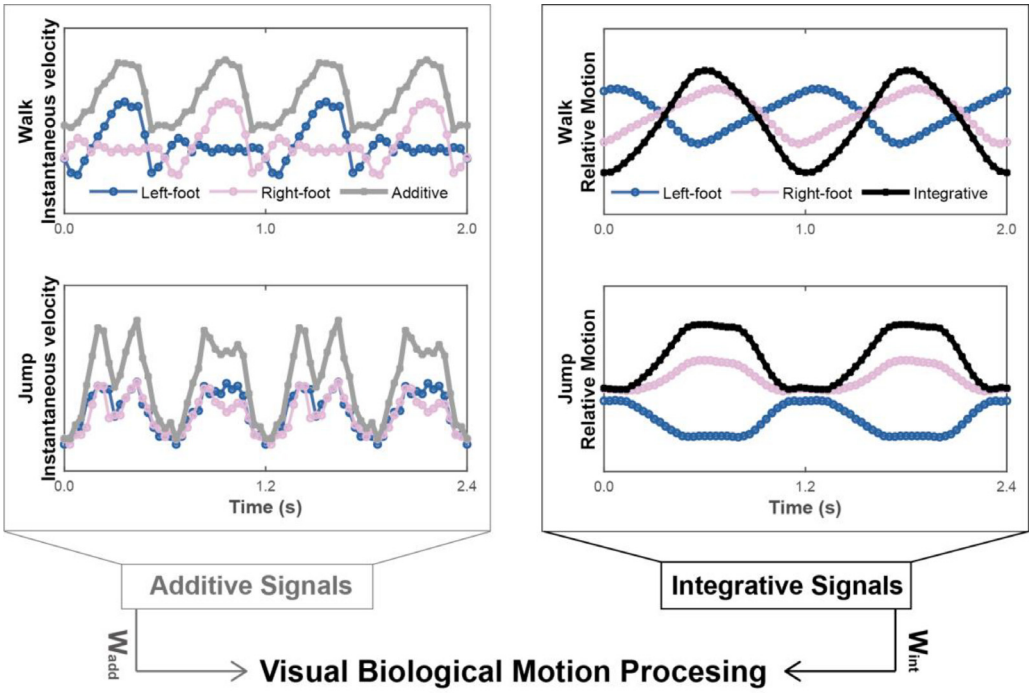

Fig. 2. The additive signals and integrative signals generated based on the Walk (upper panel) and Jump (lower panel) BM sequences. The additive signals (gray lines) are depicted as the instantaneous velocity, i.e., Euclidian displacement at each time point, accumulated across the two feet over time. Red and blue lines in the left panel indicate the velocity profile of the left and right feet, respectively. The integrative signals (black lines) are defined by the relative motion of the two feet, quantified as the horizontal distance between the two feet at each time point. The red and blue lines in the right panel depict the displacement of each foot in the horizontal direction. Additive and integrative signals contribute to the neural encoding of BM information with different weights (W_{add} and W_{int}).

specific entrainment effect were significantly correlated with those in the task performance (i.e., detection sensitivity) across all the experiments.

2.6. Modeling

The critical visual features of BM are carried by the movements of multiple joints over time rather than any single point in time or the motion of one joint in space. Therefore, the cortical tracking of rhythmic structures in BM information may involve the neural encoding of spatiotemporally summated BM signals. Here we constructed two possible summation signals, namely, the additive signal and the integrative signal (Fig. 2), based on different summation rules.

The additive signal is formed by the linear addition of kinematic cues across individual joints at each time stamp. Given the significant role of motion velocity in visual BM perception (Cai et al., 2011; Faivre and Koch, 2014; Thurman and Grossman, 2008), this signal (S_{add}, Eq.1; Fig. 2, left panel, gray lines), in its simplest form, can be quantified by the summation of velocity series across the most representative bilateral joints, i.e., the left and right feet (Bardi et al., 2014; Troje and Westhoff, 2006; Wang et al., 2014):

$$S_{add}(t) = V_L(t) + V_R(t) \quad (1)$$

V_L and V_R denote the instantaneous velocity of the left and right feet over time, respectively. The velocity at each time point t (corresponding to an individual frame) was computed as the Euclidian displacement of each foot from the current frame to the next frame.

The integrative signal results from the integration of the opponent motion pattern of the bilateral limbs. It reflects a specific organization principle to integrate bilateral limbs into a unitary object when dealing with complex non-rigid motion signals (Booth et al., 2002; Casile and Giese, 2005; Giese and Poggio, 2003). To be simplified but remain its core information, the integrative signal (S_{int}, Eq.2; Fig. 2, right panel, black lines) was quantified by the relative motion (i.e., horizontal distance) of bilateral feet, consistent with the definition of opponent motion in previous studies (Casile and Giese, 2005; Thurman and Grossman, 2008).

$$S_{int}(t) = H_L(t) - H_R(t) \quad (2)$$

H_L and H_R denote horizontal displacement signals of left and right feet over time, respectively. Their difference per frame characterizes the relative motion of two feet at each time point t. S_{int} with a value of zero indicates the moment of legs crossing.

To estimate the contributions of the additive signals and integrative signals to the orientation-dependent neural representation of BM, we assigned independent weights (W_{add} and W_{int}) to these two signals, then combined the weighted signals and transformed them into the frequency domain through the fast Fourier transformation:

$$Sf = F(W_{add} \times S_{add} + W_{int} \times S_{int}) \quad (3)$$

W_{add} represents the weight of additive signals, and W_{int} represents the weight of integrative signals. *F* is the transformation process performed based on the MATLAB *fft* function.

We fit the frequency transformed signals (Sf) with the observed spectral distribution of neural oscillations and minimized their rooted mean squared error (RMSE) through a constrained optimization algorithm (MATLAB *fmincon*). The only parameters available to vary were W_{add} and W_{int}, which were constrained above zero to evaluate the contribution of each signal to the neural encoding of BM information. We estimated the model parameters for each condition and participant within the 0–2.3 frequency band. The set of optimized parameter values minimizing the rooted mean squared error (RMSE) between the observed spectral data and the model predicted data was selected as the best estimate. The optimization started from 900 sets of possible parameter values in the linear parameter space to avoid being trapped in a local minimum.

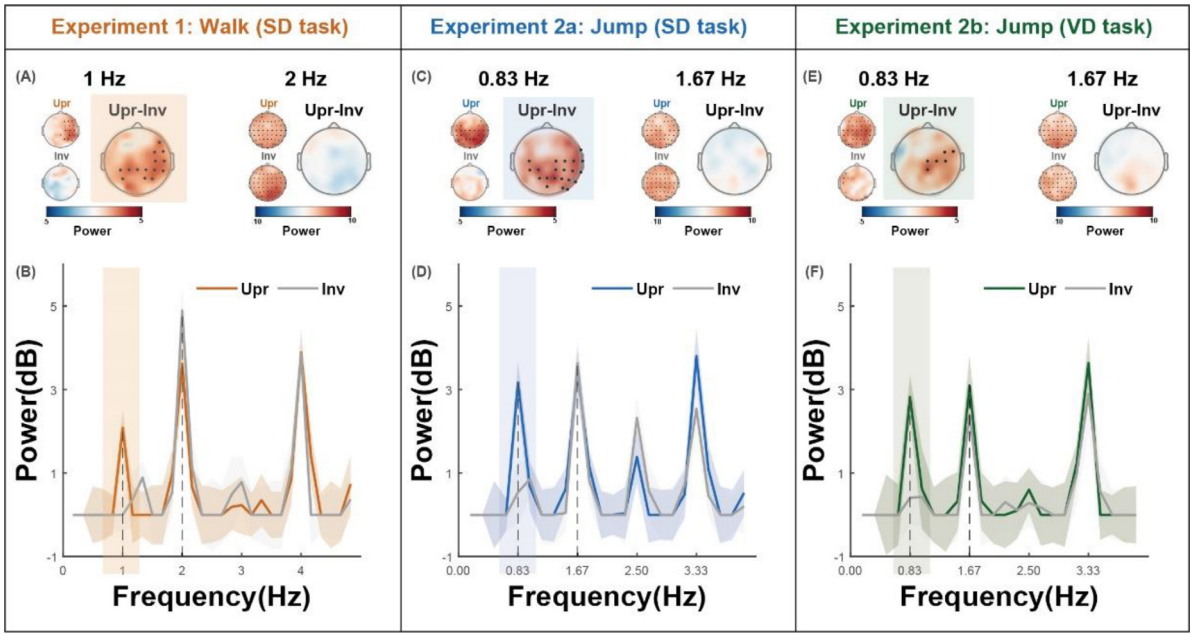

Fig. 3. Cortical tracking of the rhythmic kinematic structures in BM stimuli. (A) The scalp topographies for the neural entrainment effect at the higher-level (1 Hz) and basic-level (2 Hz) cycle frequencies for each condition: upright (Upr) or inverted (Inv), and for the contrast between these conditions (Upr-Inv) in Experiment 1. Black dots indicate electrodes showing a significant spectral peak in the upright or inverted condition, or a significant inversion effect, as revealed by the cluster-based permutation test. **(B)** Power spectra averaged across the channels in the cluster showing a significant inversion effect. Shaded regions indicate standard errors of the mean. **(C) & (D)** show topographic and spectral power results for Experiment 2a and **(E) & (F)** for Experiment 2b. SD: speed detection; VD: variation detection.

3. Results

3.1. Cortical tracking of hierarchical rhythmic structures in BM stimuli

In Experiment 1, participants watched the motion sequences of upright and inverted point-light walkers and were required to detect their speed changes while their EEG signals were simultaneously recorded. We first examined whether the power responses at the two frequencies of interest (1 Hz for the gait cycle and 2 Hz for the step cycle) were greater than zero, respectively, using a cluster-based permutation test (Maris and Oostenveld, 2007). At 1 Hz, we observed a cluster showing a significant entrainment effect or spectral peak in the upright ($p < 0.001$) but not in the inverted condition (Fig. 3A). At 2 Hz, both upright ($p = 0.002$) and inverted ($p < 0.001$) stimuli elicited a significant entrainment effect almost over the whole brain. To further investigate the BM-specific neural responses, we compared power responses between the upright and inverted conditions at the two frequencies of interest, respectively, and found a significant cluster only at 1 Hz (Fig. 3A; $p = 0.003$; P3, P2, P4, CP3, CP1, CPZ, CP2, CP4, CP6, C4, C6, FC4, FC6, F6), in which the average power across participants was stronger in the upright condition compared with the inverted condition. Such an inversion effect was right-lateralized, and pronounced over the right parieto-temporal region. The power spectra results pooled over channels within this significant cluster are shown in Fig.3B. By contrast, no significant inversion effect was observed at 2 Hz for the step-cycle frequency (Fig. 3A).

Together, these results revealed two important spectral components, i.e., enhanced neural oscillations at 1-Hz and 2-Hz, involved in the cortical tracking of the rhythmic structures in the BM stimuli. Critically, the spectral power at 1 Hz was specifically enhanced for upright BM stimuli relative to the inverted counterparts, suggesting that the neural tracking of higher-level rhythmic structures is associated with the specific neural representation of BM signals.

3.2. Cortical tracking of BM signals independent of motion type, speed, and task

Experiment 2a aimed to investigate whether the findings from Experiment 1 can be generalized to different motion types and speeds. To address this issue, we employed point-light jumpers with a different motion speed (0.83 Hz for the jump cycle) from the point-light walkers as the experimental stimuli. In Experiment 2b, we adopted a frequency-irrelevant variation detection task (i.e., VD task, see Methods) to further explore whether the entrainment effect could occur with different task demands.

In Experiments 2a & 2b, we performed the same statistical analysis as Experiment 1 and found similar results. In Experiment 2a, we obtained a cluster with a significant entrainment effect in the upright condition ($p < 0.001$, cluster-based permutation test) but not in the inverted condition at 0.83 Hz (Fig. 3C). At 1.67 Hz, both upright and inverted stimuli elicited a significant entrainment effect widely across the brain ($ps < 0.001$). We observed similar results in Experiment 2b ($ps < 0.001$), except that there was a small left-lateralized cluster showing an entrainment effect at 0.83 Hz in the inverted condition (Fig. 3E; $p = 0.002$), probably because different task demands lead to variations in the topographical maps. More importantly, we consistently identified clusters showing significant inversion effects only at the higher-level structure frequency (i.e., 0.83 Hz) in both experiments, regardless of whether the participants were required to detect the change of speed in Experiment 2a (Fig. 3C; $p < 0.001$; T8, TP8, FT8, P1, PZ, P2, P4, P6, P8, C3, C2, C4, C6, CP3, CP1, CP2, CP4, CP6, POZ, PO6, PO8) or the frequency-irrelevant variation in Experiment 2b (Fig. 3E; $p = 0.016$; CPZ, CZ, C2, C4, FC4, FC6). The power spectra results pooled over channels within these clusters are depicted in Fig.3D and Fig.3F. In contrast, we did not find any cluster showing significant inversion effects at the basic-level rhythmic cycle frequency (i.e., 1.67 Hz) in both experiments. These results confirmed that the cortical tracking of the higher-level

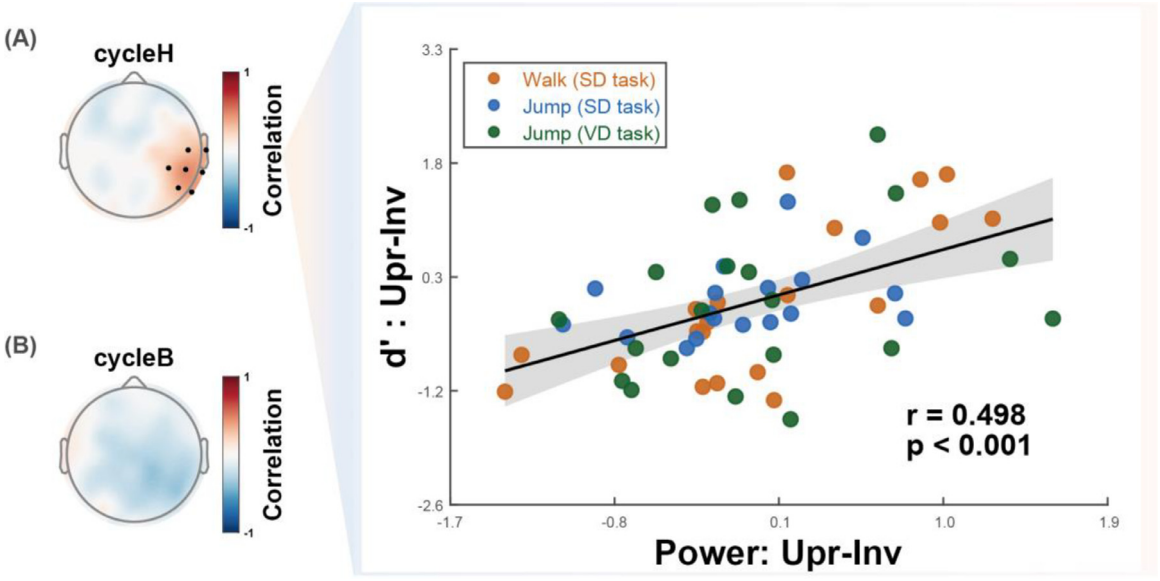

Fig. 4. The correlation between neural responses and behavioral performances. (A) The topography depicts the behavior-neuro correlation coefficients based on data collapsed across three experiments. Black dots indicate significant channels revealed by the cluster-based permutation test. Orange, blue, and green dots in the scatter plot indicate the individual data from Experiments 1, 2a, & 2b, respectively. Shaded regions indicate the 95% confidence interval. **(B)** The topography shows that the entrainment effect at the basic-level cycle frequency did not correlate with the behavioral performance at any electrode.

rhythmic structures reflects the specialized neural representation of BM signals.

Besides power, the phase-locking neural response is also a great index for the neural encoding of rhythmic information, as suggested by language studies (Ding et al., 2017; Luo and Ding, 2020). Thus, we analyzed the inter-trial phase coherence (ITPC) of the EEG data for Experiments 1, 2a, and 2b, respectively (see Supplementary Information for details). But notably, rhythmic signals in BM derive from a series of joints, which move at the same frequency but are not necessarily in a coherent phase. Specifically, the counter-phase properties of the opposite limbs in some types of BM (such as walking) may attenuate phase-locking responses at the level of neuronal populations, if we assume the EEG signals reflect phase coherence among neurons tracking different joints. Compatible with this assumption, we observed weak phase-locking neural activity for walking in Experiment 1 (see **Fig. S1** in Supplementary Information). Nevertheless, the ITPC results in Experiments 2a & 2b (**Fig. S1**) were similar to those obtained from power analysis, providing substantial evidence that the jumping stimulus, which has partial phase coherence across different joints, induces BM-specific phase-locking neural responses.

3.3. Cortical tracking of higher-level rhythmic structures correlates with behavioral performance

Across all experiments, the neural tracking effect at the higher-level structure frequency was overall stronger in the upright condition versus the inverted condition but had a wide range of individual variations. Could such variations predict observers' perceptual sensitivity to BM stimuli in the behavioral tasks? To explore this possibility, we performed a cluster-based permutation test on the Pearson correlation (Maris and Oostenveld, 2007) between the power of the neural response at each electrode and the perceptual sensitivity measured by *d'* (Green and Swets, 1966).

We transformed the inversion effects in neural responses and perceptual sensitivity (i.e., the difference between upright and inverted conditions) to Z scores for each experiment, respectively, and collapsed the data across three experiments to improve the robustness of the correlation analysis. Two outliers whose behavioral performances exceeded 2.5 standard deviations were excluded from further analysis. The topography in Fig. 4A depicted the neuro-behavior correlation coefficients over the whole brain, with a significant cluster around the right temporal-parietal electrodes ($p = 0.014$, cluster-based permutation test; T8, TP8, P6, P8, C6, CP4, CP6). As illustrated in the scatter plot, the inversion effect in neural responses at the higher-level cycle (cycleH) frequencies (averaged across channels in the significant cluster) positively correlated with the inversion effect in perceptual sensitivities ($r = 0.498$, $p < 0.001$). We did not observe any significant cluster showing positive correlation between the neural responses at the basic-level structure (cycleB) frequencies and behavioral performances (Fig. 4B).

3.4. Integrative signals contribute to the BM-specific neural encoding mechanism

Based on the EEG results, we further explored the encoding mechanism for the BM-specific cortical entrainment effects by adopting a computational modeling approach. The perceptual sensitivity to BM signals increases with the exposure time and the number of displayed joints, suggesting that the processing of rhythmic BM information relies on spatiotemporal summation (Neri et al., 1998). As described in the Methods section (see *Modeling*), the spatiotemporal summation of BM information may engage the cortical tracking of additive signals or/and integrative signals. It is plausible to assume that neural oscillations tracking a summation signal with greater weight in the upright than in the inverted condition would reflect the specialized neural representation of BM.

Therefore, we estimated the weights for the additive and integrative signals (W_{add} and W_{int}) to evaluate their separate contributions to the neural encoding of BM information. Here, we only presented the results for Experiment 1 and Experiment 2a, given that Experiment 2a & 2b used the same stimuli and yielded similar modeling results.

We fit the model data and the observed spectral distribution of neural responses for each condition and participant (Fig. 5A & C). A paired *t*-test revealed no significant effect of orientation for the RMSE (Walk: $t(19) = 0.075$, $p = 0.941$, Cohen's $d = 0.017$; $BF_{10} = 0.233$; Jump: $t(19) = 1.001$, $p = 0.330$, Cohen's $d = 0.224$; $BF_{10} = 0.362$), demonstrating that the modeling methods result in comparable fitting quality for the upright and inverted conditions. We further performed a repeated measures ANOVA on the computational modeling results, with signal type (additive vs. integrative) and stimulus orientation (upright

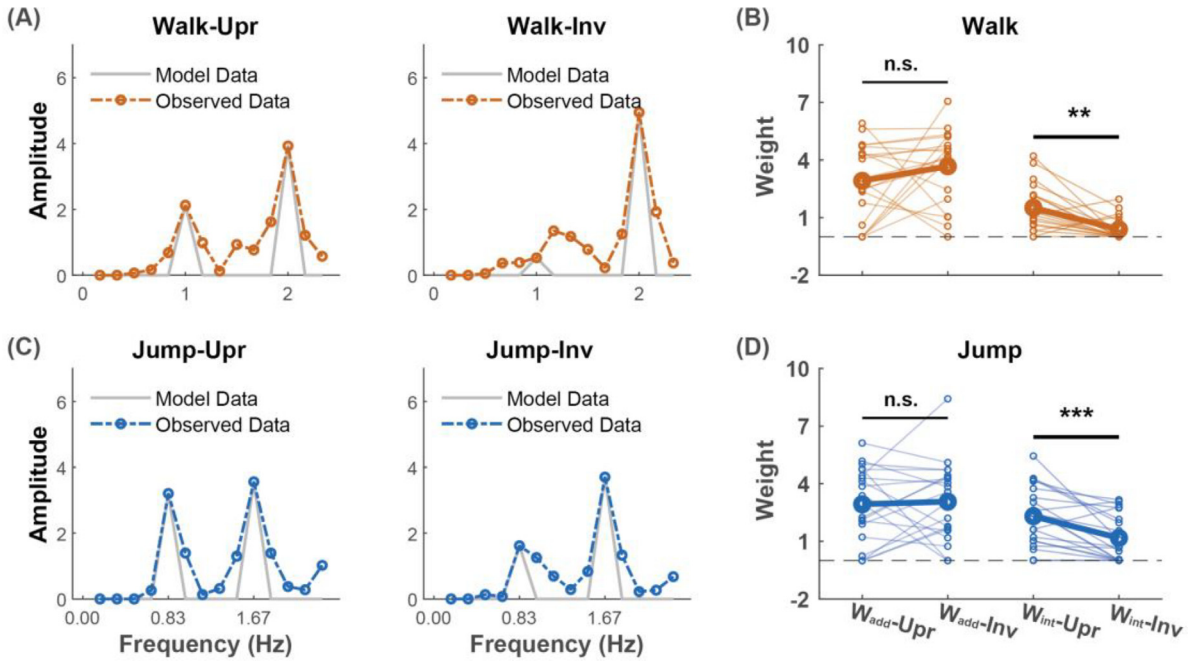

Fig. 5. Modeling results. (A) & (C) The observed and modeling data for the walk and jump stimuli. Colored dashed lines refer to the spectral distribution within the 0–2.3 Hz frequency band in the group-level EEG response to upright (left panel) or inverted (right panel) stimuli. Gray solid lines represent the predicted data generated by the model. **(B) & (D)** Estimated W_{add} and W_{int} values for each orientation condition and stimulus type. Light lines and circles indicate individual data. Bold lines and circles indicate the group means. W_{add}: the estimated weight of additive signals; W_{int}: the estimated weight of integrative signals; n.s.: not significant; **: $p < 0.01$; ***: $p < 0.001$.

vs. inverted) as within-subject variables, for the walk and jump stimuli, respectively. For both stimuli, the main effect of signal type was significant (Walk: F (1,19) = 50.200, $p < 0.001$, $\eta^2 = 0.725$; Jump: F (1,19) = 13.026, $p = 0.002$, $\eta^2 = 0.407$), with a higher weight for additive than for integrative signals. No significant main effect of orientation was observed (Walk: F (1,19) = 0.353, $p = 0.560$, $\eta^2 = 0.018$; Jump: F (1,19) = 3.109, $p = 0.094$, $\eta^2 = 0.141$). Most importantly, the interaction between orientation and signal type was significant (Walk: F (1,19) = 6.534, $p = 0.019$, $\eta^2 = 256$; Jump: F (1,19) = 4.904, $p = 0.039$, $\eta^2 = 205$). The post-hoc comparisons with Bonferroni correction showed that the weight for additive signals was not significantly different between the upright and inverted conditions (Walk: t (19) = −1.227, $p = 1.000$, Cohen's $d = 0.274$, $BF_{10} = 0.448$; Jump: t (19) = −0.267, $p = 1.000$, Cohen's $d = 0.060$, $BF_{10} = 0.240$), while that for integrative signals was significantly larger in the upright than in the inverted condition (Fig. 5 B& D, Walk: t (19) = 3.840, $p = 0.007$, Cohen's $d = 0.859$, $BF_{10} = 33.573$; Jump: t (19) = 3.920, $p = 0.006$, Cohen's $d = 0.877$, $BF_{10} = 39.332$). These results suggest that the cortical tracking of integrative rather than additive signals is related to the specialized neural representation and visual processing of BM information.

4. Discussion

The current study investigates how oscillatory brain activity dynamically encodes rhythmic signals in human movements and supports the visual processing of BM information. We found that neural oscillations entrained to the basic- and higher-level spatiotemporal structures emerged from periodic kinematic profiles of the BM sequences. More importantly, the cortical tracking of higher-level kinematic structures of the BM stimuli (such as the gait cycle and jump cycle) showed a significant inversion effect, manifested by enhanced neural responses to upright over inverted BM signals. Such inversion effect consistently appeared across stimulus types and tasks and was positively correlated with individuals' perceptual sensitivity to the BM stimuli. Since inversion does not change the low-level physical attributes but abolishes the critical kinematic features of BM (Troje and Westhoff, 2006; Vallortigara and Regolin, 2006; Wang et al., 2022), these findings hint at a unique temporal coding mechanism for visual BM processing.

The modeling results further suggest that although both additive and integrative signals contribute to the perception of BM, the integrative signals depicting the complex opponent motion pattern appear to drive the orientation-dependent, BM-specific neural encoding process. A possible explanation for these findings is that upright BM stimuli convey gravity-compatible kinematic cues that are critical for BM perception (Maffei et al., 2015; Shi et al., 2010; Vallortigara and Regolin, 2006; Wang et al., 2010, 2014; Wang and Jiang, 2012; Wang et al., 2022). Such gravity-compatible motion cues have been extremely familiar to terrestrial creatures on earth. Hence, they make up a sort of "vocabulary" for developing dynamic templates in the brain to trigger the processing of integrative signals contained in upright BM stimuli (Cavanagh et al., 2001). However, when confronting inverted BM stimuli that do not activate the gravity-compatible dynamic templates, the brain may only utilize the additive signals for visual motion processing. Further research could examine this hypothesis by isolating or depriving the gravity-compatible signals from BM stimuli (Chang et al., 2018).

Our findings extend our understanding of the temporal dynamic characteristics of the neural representation of BM information. Previous event-related potentials (ERP) studies have revealed that upright BM stimuli, compared with inverted BM, elicit stronger negative neural responses (e.g., N170, N2, N300) over the occipitotemporal region (Jokisch et al., 2005; White et al., 2014). However, these negative components may reflect the neural processing of configurational rather than kinematic cues. On the one hand, intact BM stimuli always elicit a stronger negative response than spatially scrambled ones (Bottari et al., 2015; Hirai et al., 2003, 2013; Hirai and Hiraki, 2005; Krakowski et al., 2011; Saunier et al., 2013). On the other hand, the strength of the negative neural response is unable to distinguish between intact and temporally scrambled BM stimuli (Hirai and Hiraki, 2006). Contrary to these findings, our study reveals an oscillatory brain mechanism engaging in selective tracking of the critical kinematic features of BM signals. Such a

mechanism may support the spatiotemporal integration of BM information and provides a temporal frame for the segmentation of BM signals, laying the ground for further elaborate analysis of dynamic characteristics of the BM stimuli in the brain.

Notably, the BM-specific cortical tracking effect and the neurobehavioral correlation observed in the current study are lateralized to the right parieto-temporal area. These findings are in line with observations from functional magnetic resonance imaging (fMRI) and transcranial magnetic stimulation (TMS) studies regarding the hemispheric asymmetry in visual BM processing. In particular, the right posterior superior temporal sulcus (pSTS) shows stronger activity or a different activation pattern of fMRI signals in response to BM compared with non-BM or inverted BM stimuli (Grossman and Blake, 2001; Wang et al., 2022). Repetitive TMS over the right pSTS disrupts the perception of upright but not inverted BM (Grossman et al., 2005). This region is also responsible for the integration of kinematic and configurational cues in BM information (Jastorff et al., 2012; Jastorff and Orban, 2009; Sokolov et al., 2018). Considering the crucial role of pSTS in the specialized representation of BM signals and the spatiotemporal integration of BM information, it is likely that the cortical tracking of the higher-level rhythmic structures in BM signals originates from this region. In addition, we also observed the cortical tracking of BM signals on the central electrodes. Previous research has found critical contribution of motor regions to BM processing (Fraiman et al., 2014; Martins et al., 2017; Pozzo et al., 2017; Saygin, 2007; Saygin et al., 2004; Ulloa and Pineda, 2007; van Kemenade et al., 2012), with a causal relationship between premotor areas and BM perception (Saygin, 2007; van Kemenade et al., 2012). Thus, although we did not find a significant behavioral-neural correlation in the central region, this region remains a possible candidate for the cortical tracking response. Future research could pinpoint the exact neural substrates for encoding rhythmic BM signals using an approach with high spatial and temporal resolutions, such as magnetoencephalography (MEG) combined with fMRI.

Interestingly, the superior perceptual processing in the upright orientation is a general principle that applies to various visual stimuli besides BM, such as faces, words, and other objects of expertise (Campbell and Tanaka, 2018; Gauthier et al., 1999; Kao et al., 2010; Yin, 1969; Yovel and Kanwisher, 2005), indicating there might be specialized neural circuitry for such processes. For static stimuli, the configurational processing of different visual categories and the related inversion effects occur primarily at some domain-specific cortical regions, which anatomically and functionally cluster on the fusiform gyrus of the ventral temporal cortex (Grill-Spector and Weiner, 2014; Kao et al., 2010; Watson et al., 2016; Weiner and Zilles, 2016; Yovel and Kanwisher, 2005). By contrast, the inversion effect for BM may stem from the pSTS, a region sensitive to facial and bodily movement, and its functional connectivity with the posterior insula, an area responsible for gravity-constrained visual motion processing (Grossman et al., 2005; Grossman and Blake, 2001; Wang et al., 2022). The current study further suggests that the orientation-dependent neural representation of BM relates to cortical tracking of its kinematic structure, presumably driven by oscillatory neural responses transmitted through the dorsal visual stream to the pSTS. These findings, taken together, indicate that there might be specialized and distinct neural circuits underlying the inversion effects for dynamic and static visual objects, respectively.

Like BM, music and languages convey nested rhythmic information generated by human activities. More intriguingly, the hierarchical cortical tracking of BM functionally resembles that of music and speech, despite these processes arising from different sensory modalities. Studies on music perception demonstrate selective neural entrainment to lower-level (e.g., beat/time/pulse) and higher-level (e.g., meter) rhythmic structures, which reflects the internal representation of music rather than the acoustic energy of the sound envelope (Lenc et al., 2018; Nozaradan, 2014; Nozaradan et al., 2011, 2012). Among these, the higher-level cortical tracking effect is modulated by top-down metric interpretation of the beat (Nozaradan et al., 2011) and one's music experience (Cirelli et al., 2016; Doelling and Poeppel, 2015; Soley and Hannon, 2010). In speech processing, while cortical oscillations entrain to both higher- (e.g., phrase) and lower- (e.g., syllable) level rhythmic linguistic structures, the former effect is more relevant to speech perception and comprehension (Ding et al., 2016, 2017; Keitel et al., 2018; Luo and Ding, 2020). Here, we found hierarchical neural entrainment to rhythmic BM, with only the cortical tracking of higher-level kinematic structures (i.e., the walk and jump cycle) reflecting the BM-specific neural processing and correlated with perceptual sensitivity. The similarity among music, speech, and BM sheds light on how our cognitive and neural systems process rhythmic information in these complex and meaningful dynamic stimuli. Humans and various other species possess the ability to produce, perceive, and respond to rhythmic signals, either in the form of sounds or actions (Kotz et al., 2018; Patel et al., 2009; Rouse et al., 2021). It is tempting to speculate that, when confronted with such information, it is an evolutionarily optimal response of our rhythmic brain to extract statistical regularities from the rhythmic structures embedded therein, which creates a basis for understanding others' activities and facilitating interaction. On the other hand, speech and music comprehension rely on auditory processing and learning (Cirelli et al., 2016; Ding et al., 2016; Doelling and Assaneo, 2021; Soley and Hannon, 2010), whereas BM perception, especially the processing of its kinematic properties, is an innate capability of the visual system less dependent on learned experience (Bardi et al., 2011; Chang and Troje, 2009; Simion et al., 2008; Vallortigara and Regolin, 2006; Wang et al., 2018). It would be interesting to explore in the future whether the ability to encode the higher-order kinematic structure in BM emerges in a different way from that for speech and music through cross-species and behavioral genetic research.

5. Conclusion

Evolution has endowed biological organisms with the ability to interact in real-time with external signals that rhythmically stimulate their sensory organs (Hattori and Tomonaga, 2020; Kotz et al., 2018). The current study adds to this picture by showing that the cortical neural oscillations dynamically and hierarchically represent rhythmic signals in human body movements. Crucially, the neural encoding of spatiotemporally integrated kinematic cues (i.e., opponent motions of bilateral limbs) embedded in higher-level motion structures supports the specialized visual processing of BM information. These findings provide fresh insights into the dynamic neural encoding mechanism underlying visual BM processing and open the possibility of treating the cortical tracking of rhythmic kinematic structures as a biomarker for visual BM perception.

Data and code accessibility statement

The processed data analyzed during the study and the Matlab code for generating the figures are available at http://ir.psych.ac.cn/handle/311026/42945.

Conflict of interest

The authors declare no conflicts of interest.

Credit authorship contribution statement

Li Shen: Conceptualization, Methodology, Software, Formal analysis, Investigation, Visualization, Writing – original draft. **Xiqian Lu:** Writing – original draft. **Xiangyong Yuan:** Methodology, Writing – original draft. **Ruichen Hu:** Investigation. **Ying Wang:** Conceptualization, Methodology, Supervision, Writing – review & editing. **Yi Jiang:** Supervision, Writing – review & editing.

Acknowledgments

This research was supported by grants from the Ministry of Science and Technology of China (STI2030-Major Projects 2021ZD0203800 and 2021ZD0204200), the National Natural Science Foundation of China (Nos. 32171059 and 31830037), the Strategic Priority Research Program (No. XDB32010300), the Interdisciplinary Innovation Team (JCTD-2021-06), the Youth Innovation Promotion Association of the Chinese Academy of Sciences, the Scientific Foundation of Institute of Psychology, Chinese Academy of Sciences (No. E2CX4325CX), and the Fundamental Research Funds for the Central Universities.

Supplementary materials

Supplementary material associated with this article can be found, in the online version, at doi:10.1016/j.neuroimage.2023.119893.

References

Bardi, L., Regolin, L., Simion, F., 2011. Biological motion preference in humans at birth: role of dynamic and configural properties. Dev. Sci. 14 (2), 353–359. doi:10.1111/j.1467-7687.2010.00985.x.

Bardi, L., Regolin, L., Simion, F., 2014. The first time ever I saw your feet: inversion effect in Newborns' sensitivity to biological motion. Dev. Psychol. 50 (4), 986–993. doi:10.1037/a0034678.

Beintema, J.A., Oleksiak, A., van Wezel, R.J.A., 2006. The influence of biological motion perception on structure-from-motion interpretations at different speeds. J. Vis. 6 (7), 712–726. doi:10.1167/6.7.4.

Bell, A.J., Sejnowski, T.J., 1995. An information-maximization approach to blind separation and blind deconvolution. Neural Comput. 7 (6), 1129–1159. doi:10.1162/neco.1995.7.6.1129.

Blake, R., Shiffrar, M., 2007. Perception of human motion. Annu. Rev. Psychol. 58 (1), 47–73. doi:10.1146/annurev.psych.57.102904.190152.

Booth, A., Bertenthal, B., Pinto, J., 2002. Perception of the symmetrical patterning of human gait by infants. Dev. Psychol. 38(4), 554–563. doi:10.1037//0012-1649.38.4.554.

Bottari, D., Troje, N.F., Ley, P., Hense, M., Kekunnaya, R., Röder, B., 2015. The neural development of the biological motion processing system does not rely on early visual input. Cortex 71, 359–367. doi:10.1016/j.cortex.2015.07.029.

Brainard, D.H. (1997). The Psychophysics Toolbox. Spatial Vision, 10(4), 433–436.

Brookshire, G., Lu, J., Nusbaum, H.C., Goldin-Meadow, S., Casasanto, D., 2017. Visual cortex entrains to sign language. Proc. Natl. Acad. Sci. 114 (24), 6352–6357. doi:10.1073/pnas.1620350114.

Cai, P., Yang, X., Chen, L., Jiang, Y., 2011. Motion speed modulates walking direction discrimination: the role of the feet in biological motion perception. Chin. Sci. Bull. 56 (19), 2025–2030. doi:10.1007/s11434-011-4528-6.

Campbell, A., Tanaka, J.W., 2018. Inversion impairs expert budgerigar identity recognition: a face-like effect for a nonface object of expertise. Perception 47 (6), 647–659. doi:10.1177/0301006618771806.

Casile, A., Giese, M.A., 2005. Critical features for the recognition of biological motion. J. Vis. 5 (4), 348–360. doi:10.1167/5.4.6.

Cavanagh, P., Labianca, A.T., Thornton, I.M., 2001. Attention-based visual routines: sprites. Cognition 80 (1), 47–60. doi:10.1016/S0010-0277(00)00153-0.

Chang, D.H.F., Ban, H., Ikegaya, Y., Fujita, I., Troje, N.F., 2018. Cortical and subcortical responses to biological motion. Neuroimage 174, 87–96. doi:10.1016/j.neuroimage.2018.03.013.

Chang, D.H.F., Troje, N.F., 2008. Perception of animacy and direction from local biological motion signals. J. Vis. 8 (5), 3. doi:10.1167/8.5.3.

Chang, D.H.F., Troje, N.F., 2009. Acceleration carries the local inversion effect in biological motion perception. J. Vis. 9 (1), 1–17. doi:10.1167/9.1.19, 19.

Cirelli, L.K., Spinelli, C., Nozaradan, S., Trainor, L.J., 2016. Measuring neural entrainment to beat and meter in infants: effects of music background. Front. Neurosci. 10, 299. doi:10.3389/fnins.2016.00229.

Delorme, A., Makeig, S., 2004. EEGLAB: an open source toolbox for analysis of single-trial EEG dynamics including independent component analysis. J. Neurosci. Methods 134 (1), 9–21. doi:10.1016/j.jneumeth.2003.10.009.

Ding, N., Melloni, L., Yang, A., Wang, Y., Zhang, W., Poeppel, D., 2017. Characterizing neural entrainment to hierarchical linguistic units using electroencephalography (EEG). Front. Hum. Neurosci. 11, 481. doi:10.3389/fnhum.2017.00481.

Ding, N., Melloni, L., Zhang, H., Tian, X., Poeppel, D., 2016. Cortical tracking of hierarchical linguistic structures in connected speech. Nat. Neurosci. 19 (1), 158–164. doi:10.1038/nn.4186.

Doelling, K.B., Assaneo, M.F., 2021. Neural oscillations are a start toward understanding brain activity rather than the end. PLoS Biol. 19 (5), e3001234. doi:10.1371/journal.pbio.3001234.

Doelling, K.B., Poeppel, D., 2015. Cortical entrainment to music and its modulation by expertise. Proc. Natl. Acad. Sci. 112 (45), E6233–E6242. doi:10.1073/pnas.1508431112.

Faivre, N., Koch, C., 2014. Temporal structure coding with and without awareness. Cognition 131 (3), 404–414. doi:10.1016/j.cognition.2014.02.008.

Fraiman, D., Saunier, G., Martins, E.F., Vargas, C.D., 2014. Biological motion coding in the brain: analysis of visually driven EEG functional networks. PLoS ONE 9 (1), e84612. doi:10.1371/journal.pone.0084612.

Gauthier, I., Tarr, M.J., Anderson, A.W., Skudlarski, P., Gore, J.C., 1999. Activation of the middle fusiform "face area" increases with expertise in recognizing novel objects. Nat. Neurosci. 2 (6), 568–573. doi:10.1038/9224.

Giese, M.A., Poggio, T., 2003. Neural mechanisms for the recognition of biological movements. Nat. Rev. Neurosci. 4 (3), 179–192. doi:10.1038/nrn1057.

Green, D.M., Swets, J.A., 1966. Signal Detection Theory and Psychophysics. Wiley, New York.

Grill-Spector, K., Weiner, K.S., 2014. The functional architecture of the ventral temporal cortex and its role in categorization. Nat. Rev. Neurosci. 15, 536–548. doi:10.1038/nrn3747.

Grossman, E.D., Battelli, L., Pascual-Leone, A, 2005. Repetitive TMS over posterior STS disrupts perception of biological motion. Vis. Res. 45 (22), 2847–2853. doi:10.1016/j.visres.2005.05.027.

Grossman, E.D., Blake, R., 2001. Brain activity evoked by inverted and imagined biological motion. Vis. Res. 41 (10–11), 1475–1482. doi:10.1016/S0042-6989(00)00317-5.

Hattori, Y., Tomonaga, M., 2020. Rhythmic swaying induced by sound in chimpanzees. Proc. Natl. Acad. Sci. 117 (2), 936–942. doi:10.1073/pnas.1910318116.

Hirai, M., Fukushima, H., Hiraki, K., 2003. An event-related potentials study of biological motion perception in humans. Neurosci. Lett. 344 (1), 41–44. doi:10.1016/S0304-3940(03)00413-0.

Hirai, M., Hiraki, K., 2005. An event-related potentials study of biological motion perception in human infants. Cogn. Brain Res. 22 (2), 301–304. doi:10.1016/j.cogbrainres.2004.08.008.

Hirai, M., Hiraki, K., 2006. The relative importance of spatial versus temporal structure in the perception of biological motion: an event-related potential study. Cognition 99 (1), B15–B29. doi:10.1016/j.cognition.2005.05.003.

Hirai, M., Senju, A., 2020. The two-process theory of biological motion processing. Neurosci. Biobehav. Rev. 111, 114–124. doi:10.1016/j.neubiorev.2020.01.010.

Hirai, M., Watanabe, S., Honda, Y., Kakigi, R., 2013. Developmental changes in point-light walker processing during childhood: a two-year follow-up ERP study. Dev. Cogn. Neurosci. 5, 51–62. doi:10.1016/j.dcn.2013.01.002.

Jastorff, J., Orban, G.A., 2009. Human functional magnetic resonance imaging reveals separation and integration of shape and motion cues in biological motion processing. J. Neurosci. 29 (22), 7315–7329. doi:10.1523/JNEUROSCI.4870-08.2009.

Jastorff, J., Popivanov, I.D., Vogels, R., Vanduffel, W., Orban, G.A., 2012. Integration of shape and motion cues in biological motion processing in the monkey STS. Neuroimage 60 (2), 911–921. doi:10.1016/j.neuroimage.2011.12.087.

Johansson, G., 1973. Visual perception of biological motion and a model for its analysis. Percept. Psychophys. 14 (2), 201–211. doi:10.3758/BF03212378.

Jokisch, D., Daum, I., Suchan, B., Troje, N., 2005. Structural encoding and recognition of biological motion: evidence from event-related potentials and source analysis. Behav. Brain Res. 157 (2), 195–204. doi:10.1016/j.bbr.2004.06.025.

Jung, T.-.P., Makeig, S., Westerfield, M., Townsend, J., Courchesne, E., Sejnowski, T.J., 2000. Removal of eye activity artifacts from visual event-related potentials in normal and clinical subjects. Clin. Neurophysiol. 111 (10), 1745–1758. doi:10.1016/S1388-2457(00)00386-2.

Kao, C.-.H., Chen, D.-.Y., Chen, C.-.C., 2010. The inversion effect in visual word form processing. Cortex 46 (2), 217–230. doi:10.1016/j.cortex.2009.04.003.

Kayser, S., Ince, R., Gross, J., Kayser, C., 2015. Irregular speech rate dissociates auditory cortical entrainment, evoked responses, and frontal alpha. J. Neurosci. 35, 14691–14701. doi:10.1523/JNEUROSCI.2243-15.2015.

Keitel, A., Gross, J., Kayser, C., 2018. Perceptually relevant speech tracking in auditory and motor cortex reflects distinct linguistic features. PLoS Biol. 16 (3), e2004473. doi:10.1371/journal.pbio.2004473.

Kotz, S.A., Ravignani, A., Fitch, W.T., 2018. The evolution of rhythm processing. Trends Cogn. Sci. 22 (10), 896–910. doi:10.1016/j.tics.2018.08.002.

Krakowski, A.I., Ross, L.A., Snyder, A.C., Sehatpour, P., Kelly, S.P., Foxe, J.J., 2011. The neurophysiology of human biological motion processing: a high-density electrical mapping study. Neuroimage 56 (1), 373–383. doi:10.1016/j.neuroimage.2011.01.058.

Lenc, T., Keller, P.E., Varlet, M., Nozaradan, S., 2018. Neural tracking of the musical beat is enhanced by low-frequency sounds. Proc. Natl. Acad. Sci. 115 (32), 8221–8226. doi:10.1073/pnas.1801421115.

Luo, C., Ding, N., 2020. Cortical encoding of acoustic and linguistic rhythms in spoken narratives. Elife 9, e60433. doi:10.7554/eLife.60433.

Maffei, V., Indovina, I., Macaluso, E., Ivanenko, Y.P.A., Orban, G., Lacquaniti, F, 2015. Visual gravity cues in the interpretation of biological movements: neural correlates in humans. Neuroimage 104, 221–230. doi:10.1016/j.neuroimage.2014.10.006.

Makeig, S., 2002. Response: event-related brain dynamics – unifying brain electrophysiology. Trends Neurosci. 25 (8), 390. doi:10.1016/S0166-2236(02)02198-7.

Maris, E., Oostenveld, R., 2007. Nonparametric statistical testing of EEG- and MEG-data. J. Neurosci. Methods 164 (1), 177–190. doi:10.1016/j.jneumeth.2007.03.024.

Martins, E.F., Lemos, T., Saunier, G., Pozzo, T., Fraiman, D., Vargas, C.D., 2017. Cerebral dynamics during the observation of point-light displays depicting postural adjustments. Front. Hum. Neurosci. 11, 217. doi:10.3389/fnhum.2017.00217.

Neri, P., Morrone, M., Burr, D., 1998. Seeing biological motion. Nature 395, 894–896. doi:10.1038/27661.

Nozaradan, S., 2014. Exploring how musical rhythm entrains brain activity with electroencephalogram frequency-tagging. Phil. Trans. R. Soc. B 369, 20130393. doi:10.1098/rstb.2013.0393.

Nozaradan, S., Peretz, I., Missal, M., Mouraux, A., 2011. Tagging the neuronal entrainment to beat and meter. J. Neurosci. 31 (28), 10234–10240. doi:10.1523/JNEUROSCI.0411-11.2011.

Nozaradan, S., Peretz, I., Mouraux, A., 2012. Selective neuronal entrainment to the beat and meter embedded in a musical rhythm. J. Neurosci. 32 (49), 17572–17581. doi:10.1523/JNEUROSCI.3203-12.2012.

Oostenveld, R., Fries, P., Maris, E., Schoffelen, J.-M., 2011. FieldTrip: open source software for advanced analysis of MEG, EEG, and invasive electrophysiological data. Comput. Intell. Neurosci. 2011, 156869. doi:10.1155/2011/156869.

Patel, A.D., Iversen, J.R., Bregman, M.R., Schulz, I., 2009. Experimental evidence for synchronization to a musical beat in a nonhuman animal. Curr. Biol. 19 (10), 827–830. doi:10.1016/j.cub.2009.03.038.

Pavlova, M.A., 2012. Biological motion processing as a hallmark of social cognition. Cereb. Cortex 22 (5), 981–995. doi:10.1093/cercor/bhr156.

Pelli, D.G., 1997. The VideoToolbox software for visual psychophysics: transforming numbers into movies. Spat. Vis. 10 (4), 437–442.

Pozzo, T., Inuggi, A., Keuroghlanian, A., Panzeri, S., Saunier, G., Campus, C., 2017. Natural translating locomotion modulates cortical activity at action observation. Front. Syst. Neurosci. 11, 83. doi:10.3389/fnsys.2017.00083.

Riecke, L., Formisano, E., Sorger, B., Başkent, D., Gaudrain, E., 2018. Neural entrainment to speech modulates speech intelligibility. Curr. Biol. 28 (2), 161–169. doi:10.1016/j.cub.2017.11.033.

Rouse, A.A., Patel, A.D., Kao, M.H., 2021. Vocal learning and flexible rhythm pattern perception are linked: evidence from songbirds. Proc. Natl. Acad. Sci. 118 (29), e2026130118. doi:10.1073/pnas.2026130118.

Saunier, G., Martins, E.F., Dias, E.C., de Oliveira, J.M., Pozzo, T., Vargas, C.D., 2013. Electrophysiological correlates of biological motion permanence in humans. Behav. Brain Res. 236, 166–174. doi:10.1016/j.bbr.2012.08.038.

Saygin, A.P., 2007. Superior temporal and premotor brain areas necessary for biological motion perception. Brain 130 (9), 2452–2461. doi:10.1093/brain/awm162.

Saygin, A.P., Wilson, S.M., Hagler, D.J., Bates, E., Sereno, M.I., 2004. Point-light biological motion perception activates human premotor cortex. J. Neurosci. 24 (27), 6181–6188. doi:10.1523/JNEUROSCI.0504-04.2004.

Shi, J., Weng, X., He, S., Jiang, Y., 2010. Biological motion cues trigger reflexive attentional orienting. Cognition 117 (3), 348–354. doi:10.1016/j.cognition.2010.09.001.

Simion, F., Regolin, L., Bulf, H., 2008. A predisposition for biological motion in the newborn baby. Proc. Natl. Acad. Sci. 105 (2), 809–813. doi:10.1073/pnas.0707021105.

Sokolov, A.A., Zeidman, P., Erb, M., Ryvlin, P., Friston, K.J., Pavlova, M.A., 2018. Structural and effective brain connectivity underlying biological motion detection. Proc. Natl. Acad. Sci. 115 (51), E12034–E12042. doi:10.1073/pnas.1812859115.

Soley, G., Hannon, E., 2010. Infants prefer the musical meter of their own culture: a cross-cultural comparison. Dev. Psychol. 46, 286–292. doi:10.1037/a0017555.

Thurman, S.M., Grossman, E.D., 2008. Temporal "Bubbles" reveal key features for point-light biological motion perception. J. Vis. 8 (3), 28. doi:10.1167/8.3.28, 1-11.

Troje, N.F., Westhoff, C., 2006. The inversion effect in biological motion perception: evidence for a "life detector"? Curr. Biol. 16 (8), 821–824. doi:10.1016/j.cub.2006.03.022.

Ulloa, E.R., Pineda, J.A., 2007. Recognition of point-light biological motion: mu rhythms and mirror neuron activity. Behav. Brain Res. 183 (2), 188–194. doi:10.1016/j.bbr.2007.06.007.

Vallortigara, G., Regolin, L., 2006. Gravity bias in the interpretation of biological motion by inexperienced chicks. Curr. Biol. 16 (8), R279–R280. doi:10.1016/j.cub.2006.03.052.

van Kemenade, B.M., Muggleton, N., Walsh, V., Saygin, A.P., 2012. Effects of TMS over premotor and superior temporal cortices on biological motion perception. J. Cogn. Neurosci. 24 (4), 896–904. doi:10.1162/jocn_a_00194.

Vanrie, J., Verfaillie, K., 2004. Perception of biological motion: a stimulus set of human point-light actions. Behav. Res. Methods Instrum. Comput. 36 (4), 625–629. doi:10.3758/BF03206542.

Wang, L., Jiang, Y., 2012. Life motion signals lengthen perceived temporal duration. Proc. Natl. Acad. Sci. 109 (11), E673–E677. doi:10.1073/pnas.1115515109.

Wang, L., Yang, X., Shi, J., Jiang, Y., 2014. The feet have it: local biological motion cues trigger reflexive attentional orienting in the brain. Neuroimage 84, 217–224. doi:10.1016/j.neuroimage.2013.08.041.

Wang, L., Zhang, K., He, S., Jiang, Y., 2010. Searching for life motion signals: Visual search asymmetry in local but not global biological-motion processing. Psychol. Sci. 21 (8), 1083–1089. doi:10.1177/0956797610376072.

Wang, Y., Wang, L., Xu, Q., Liu, D., Chen, L., Troje, N.F., He, S., Jiang, Y., 2018. Heritable aspects of biological motion perception and its covariation with autistic traits. Proc. Natl. Acad. Sci. 115 (8), 1937–1942. doi:10.1073/pnas.1714655115.

Wang, Y., Zhang, X., Wang, C., et al., 2022. Modulation of biological motion perception in humans by gravity. Nat. Commun. 13, 2765. doi:10.1038/s41467-022-30347-y.

Watson, R., Huis In't Veld, E.M.J., de Gelder, B., 2016. The neural basis of individual face and object perception. Front. Hum. Neurosci. 10, 66. doi:10.3389/fnhum.2016.00066.

Weiner, K.S., Zilles, K., 2016. The anatomical and functional specialization of the fusiform gyrus. Neuropsychologia 83, 48–62. doi:10.1016/j.neuropsychologia.2015.06.033.

White, N.C., Fawcett, J.M., Newman, A.J., 2014. Electrophysiological markers of biological motion and human form recognition. Neuroimage 84, 854–867. doi:10.1016/j.neuroimage.2013.09.026.

Yin, R.K., 1969. Looking at upside-down faces. J. Exp. Psychol. 81, 141–145. doi:10.1037/h0027474.

Yovel, G., Kanwisher, N., 2005. The neural basis of the behavioral face-inversion effect. Curr. Biol. 15 (24), 2256–2262. doi:10.1016/j.cub.2005.10.072.

Yovel, G., O'Toole, A.J, 2016. Recognizing people in motion. Trends Cogn. Sci. 20 (5), 383–395. doi:10.1016/j.tics.2016.02.005.